JOURNAL OF SOLID STATE CHEMISTRY 110, 330–336 (1994)

New Quaternary Chalcogenides Ba*LnMQ*$_3$ (*Ln* = Rare Earth; *M* = Cu, Ag; *Q* = S, Se)

I. Structures and Grinding-Induced Phase Transition in BaLaCuQ_3

Amy E. Christuk, Ping Wu, and James A. Ibers

Department of Chemistry, Northwestern University, Evanston, Illinois 60208-3113

Received June 8, 1993; in revised form August 16, 1993; accepted August 17, 1993

The new quaternary compounds BaLaCuQ_3 (Q = S, Se) have been synthesized by the reaction of the constituent binary chalcogenides and elements at 1000°C. The crystal structures have been determined by X-ray diffraction techniques. Crystal data: BaLaCuS$_3$—space group D_{2h}^{16}-*Pnma*, M = 435.97, Z = 4, a = 11.316(2), b = 4.236(1), c = 11.724(2) Å (T = 115 K), V = 562.0(2) Å^3, $R_w(F^2)$ = 0.059 for 1051 observations and 38 variables, $R(F)$ = 0.019 for 1037 observations having $F_o^2 > 2\sigma(F_o^2)$; BaLaCuSe$_3$—space group D_{2h}^{16}-*Pnma*, M = 576.67, Z = 4, a = 11.111(4), b = 4.293(2), c = 13.830(4) Å (T = 115 K), V = 659.7(4) Å^3, $R_w(F^2)$ = 0.129 for 1385 observations and 38 variables, $R(F)$ = 0.050 for 1313 observations having $F_o^2 > 2\sigma(F_o^2)$. The BaLaCuS$_3$ structure has a three-dimensional framework with channels that accommodate barium ions. The lanthanum atoms have monocapped trigonal prismatic coordination and the copper atoms have tetrahedral coordination. BaLaCuSe$_3$ crystallizes into two phases, an α phase that is isostructural with BaLaCuS$_3$ and a layered β phase that is isostructural with Eu$_2$CuS$_3$. The layers, which are separated by Ba^{2+} ions, consist of edge-sharing octahedral chains and corner-sharing tetrahedral chains. The two structures are closely related and β-BaLaCuSe$_3$ undergoes a phase transformation to α-BaLaCuSe$_3$ upon mechanical grinding. The reverse phase transition occurs when α-BaLaCuSe$_3$ is annealed at elevated temperatures.

INTRODUCTION

The search for new complex chalcogenides has led to the synthesis and characterization of a number of new quaternary chalcogenides in this laboratory (1–8). These compounds display a wide range of structural features that can be described by the packing of metal–chalcogen polyhedra. In some of these systems (1–4), two kinds of metal atoms disorder and result in pseudoternary compounds. We anticipated that new structural features would be found if the cation disorder could be avoided through the use of elements with different coordination preferences (9). Recently, several new series of quaternary chalcogenides that contain three metal elements from different major blocks of the Periodic Table, namely, an alkali- or alkaline-earth metal, a rare-earth metal, and a main-group or transition metal, were synthesized (8, 10). These structures have crystallographically distinct sites for the three different types of metal atoms and there is no disorder. In this paper, the synthesis and crystal structures of the two new compounds BaLaCuS$_3$ and BaLaCuSe$_3$ are reported.

EXPERIMENTAL

Syntheses. The compounds BaLaCuQ_3 (Q = S, Se) were prepared by the reaction of elemental Cu (AESAR, 99.999%) and S (Alfa, 99.9995%) or Se (Aldrich, 99.999%) with the binary chalcogenides BaS (AESAR, 99.9%) or BaSe (prepared by the high-temperature stoichiometric reaction of Ba (AESAR, 99.5%) and Se) and La$_2$S$_3$ (Strem, 99.9%) or La$_2$Se$_3$ (prepared by the high-temperature reaction of La (Johnson Matthey, 99.9%) with Se). The starting materials were placed in quartz tubes that were subsequently evacuated to 10^{-5} Torr and sealed. After a preliminary study, an elemental ratio of 1 : 1 : 1 : 3 for Ba : La : Cu : Q was used. The quartz tubes were heated gradually to 500°C where they were kept for 24 hr before being successively brought to 700°C for 24 hr and 1000°C for 150 hr. The tubes were then cooled at a rate of 4°C/hr to 300°C and then the furnace was shut off. Yellow crystals of the sulfide and red crystals of the selenide had grown in the tubes. In each system semiquantitative EDAX analysis with the microprobe of a Hitachi S-570 scanning electron microscope confirmed the presence of all four elements in a ratio of approximately 1 : 1 : 1 : 3. Both compounds appear to be modestly stable in air and in water.

An alternative flux method was also used to grow single crystals of the selenide. Halide fluxes have been used in the growth of chalcogenide crystals for over a century

0022-4596/94 $6.00

(11), and recently several new quaternary chalcogenides have been crystallized from such fluxes (12, 13). In the present work, a halide flux was coupled with a high-temperature methathesis reaction between $BaBr_2$ and K_2Se_3 to circumvent the need to presynthesize BaSe. A similar approach was used (14) in the growth of $CdCr_2Se_4$ crystals from a mixture of Cd, Se, and $CrCl_3$. We have used a starting mixture of $BaBr_2$ (AESAR, 99.9%, dried at 400°C for 12 hr), La, Cu, K_2Se_3 (prepared from the stoichiometric reaction of elemental K (AESAR, 99%) and Se in liquid ammonia under an atmosphere of argon), and KBr (Strem, 99.999%). The chemicals were loaded in the ratio of one part of $BaLaCuSe_3$ to two and one-half parts of $BaBr_2$/KBr flux by weight. The flux had a $BaBr_2$:KBr molar ratio of 52:48 with a reported eutectic melting point of 609°C (15). This mixture was heated in an evacuated quartz tube to 850°C for 150 hr before being cooled at a rate of 4°C/hr to 300°C when the furnace was shut off. The product was washed with water and then was separated by filtration. The filtrate consisted of a mixture of red crystals and sintered red crystallites. EDAX experiments and precession X-ray photography on selected crystals and powder X-ray diffraction on ground crystals confirmed that the material was $BaLaCuSe_3$.

Bulk samples of $BaLaCuQ_3$ (Q = S, Se) were prepared by reactions of stoichiometric amounts of starting materials at 850°C for 6 days with an intermittent grinding. Some of these samples were then annealed at temperatures ranging from 400 to 1000°C.

Crystallographic study of $BaLaCuS_3$. A short needle-like crystal of approximate dimensions 0.04 by 0.10 by

TABLE 1
Crystal Data and Experimental Details for $BaLaCuS_3$ and $BaLaCuSe_3$

Compound	$BaLaCuS_3$	$BaLaCuSe_3$
Formula weight	435.97	576.67
Space group	D_{2h}^{16}-*Pnma*	D_{2h}^{16}-*Pnma*
a (Å)	11.316(2)	11.111(4)
b (Å)	4.236(1)	4.293(2)
c (Å)	11.724(2)	13.830(4)
V (Å^3)	562.0(2)	659.7(4)
Z	4	4
T of data collection (K)	115[a]	115[b]
Crystal vol. (mm^3)	1.1×10^{-3}	4.7×10^{-3}
Crystal shape	Plate, bounded by {010}, {101}	Plate, bounded by {010}, {103}
Radiation	Graphite monochromated, Mo$K\alpha$($\lambda(K\alpha_1$ = 0.7093 Å)	Graphite monochromated, Mo$K\alpha$($\lambda(K\alpha_1$ = 0.7093 Å)
Linear abs. coeff. (cm^{-1})	190.9	318.7
Transmission factors[c]	0.165–0.447	0.023–0.089
Detector aperture (mm)	Horizontal, 5.5; vertical, 5.5; 32 cm from crystal	Horizontal, 4.0; vertical, 3.0; 20 cm from crystal
Take-off angle (deg.)	2.5	3.0
Scan speed (deg. min^{-1})	2.0 in 2θ	4.1[d] in 2θ
Scan type	θ–2θ	ω–2θ
Scan range (deg.)	0.7° below $K\alpha_1$ to 0.9° above $K\alpha_2$	0.9° below $K\alpha_1$ to 0.9° above $K\alpha_2$
λ^{-1} sin θ, limits (Å)	0.0369–0.7366, $3° \le 2\theta$(Mo$K\alpha_1$) $\le 63°$	0.0332–0.7679, $2.7° \le 2\theta$(Mo$K\alpha_1$) $\le 66°$
Background counts	9 sec at each end of the scan	4.8 sec at each end of the scan
Data collected	$\pm h$ $\pm k$ $\pm \ell$	$\pm h$ $\pm k$ $\pm \ell$
No. of unique data including $F_o^2 < 0$	1051	1385
No. of unique data with $F_o^2 > 2\sigma(F_o^2)$	1037	1313
No. of variables	38	38
$R_w(F^2)$[e]	0.059	0.129
R [on F for $F_o^2 > 2\sigma(F_o^2)$]	0.019	0.050
Error in observation of unit weight	1.25	2.07

[a] The low-temperature system for the Picker diffractometer is based on a design by Huffman (29).
[b] The low-temperature system for the Nonius CAD4 diffractometer is from a design by Professor J. J. Bonnet and S. Askenazy and is commercially available from Soterem, Z. T. de Vic, 31320 Castanet-Tolosan, France.
[c] The analytical method was used for the absorption correction (30).
[d] Reflections with $\sigma(I)/I > 0.33$ were rescanned up to a maximum of 45 sec.
[e] $w^{-1} = \sigma^2(F_o^2) + (0.04 \times F_o^2)^2$ for $F_o^2 \ge 0$ and $w^{-1} = \sigma^2(F_o^2)$ for $F_o^2 < 0$.

0.25 mm was selected for data collection. Intensity data were collected by the θ–2θ scan technique on a Picker diffractometer controlled by a PC (16). The lattice constants were determined from least-squares analysis of the setting angles of 54 reflections in the range $38° < 2\theta$ (Mo$K\alpha_1$) $< 42°$ that had been automatically centered at 115 K. The refined cell constants and additional relevant crystal data are given in Table 1. Six standard reflections measured every 100 reflections throughout data collection showed no significant variations in intensity.

The initial data processing was carried out on a Stardent computer with programs and methods standard in this laboratory. From the systematic absences the space groups $Pn2_1a$ or $Pnma$ were possible. Data were corrected for absorption and then averaged. That the residual for averaging the reflections in Laue group mmm is 3.3% is a strong indication that the material crystallizes in the centrosymmetric space group $Pnma$. With the use of the direct methods program SHELXS (17), a solution was found in this space group. The final anistropic least-squares refinement on F_o^2 made use of all of the data; the program SHELXL-92 (18) was used. Values of the resultant R indices are 0.059 for $R_w(F^2)$ (all data) and 0.019 for $R(F)$ ($F_o^2 > 2\sigma(F_o^2)$). The highest residual electron density peak has a height about 0.6% of that of a La atom. The program package SHELXTL PC (17) was used for the ensuing molecular graphics generation.

Crystallographic study of $BaLaCuSe_3$. The crystal selected for data collection was a parallelepiped of approximate dimensions 0.12 by 0.15 by 0.26 mm. The lattice constants were determined from least-squares analysis of the setting angles of 25 reflections in the range $35° < 2\theta$ (Mo$K\alpha_1$) $< 39°$ that had been automatically centered at 115 K on a CAD4 diffractometer. The refined cell constants and additional relevant crystal data are given in Table 1. Intensity data were collected by the ω-2θ scan technique. Six standard reflections measured every 3 hr throughout data collection showed no significant variations in intensity. As for the sulfide, the space groups $Pnma$ or $Pn2_1a$ were possible from the systematic absences. However, the sulfide and selenide have significantly different cell dimensions and are not isostructural. With the direct-methods program SHELXS, a structure solution was found in the centrosymmetric space group $Pnma$. The data were corrected for absorption and then averaged; the residual for averaging is 7.4%. The final anisotropic refinement on F_o^2, performed as described above, resulted in values of 0.129 for $R_w(F^2)$ (all data) and 0.051 for $R(F)$ ($F_o^2 > 2\sigma(F_o^2)$). The highest residual electron density peak has a height about 1.7% of that of a La atom. In neither structure were there unusual trends in the goodness of fit as a function of F_o or scattering angle. The program MISSYM (19) was used to search for potential additional symmetry in these two structures. In $BaLaCuSe_3$, possible translational symmetry corresponding to an A-centered lattice, consistent with space group $Amma$, was suggested. However, this could be discounted.[1]

TABLE 2
Positional Parameters[a] and Equivalent Isotropic Displacement Parameters

Atom	x	y	z	U_{eq}^b (Å^3)
		$BaLaCuS_3$		
La	0.48904(2)	1/4	0.31890(2)	0.00524(13)
Ba	0.81672(2)	1/4	0.50661(2)	0.00565(14)
Cu	0.25375(5)	3/4	0.21001(5)	0.0079(2)
S(1)	0.22497(9)	1/4	0.29667(9)	0.0072(4)
S(2)	0.38814(8)	1/4	0.55809(8)	0.0068(4)
S(3)	0.45044(9)	3/4	0.14883(9)	0.0070(4)
		$BaLaCuSe_3$		
La	0.00928(5)	1/4	0.75986(4)	0.0129(3)
Ba	0.27147(7)	1/4	0.00454(4)	0.0148(4)
Cu	0.24126(13)	1/4	0.28334(10)	0.0164(6)
Se(1)	0.05671(10)	1/4	0.38422(6)	0.0115(5)
Se(2)	0.25537(9)	1/4	0.68031(7)	0.0102(5)
Se(3)	0.41404(10)	1/4	0.39664(7)	0.0123(5)

[a] All atoms are in Wyckoff position 4c.
[b] $U_{eq} = (1/3)\,\Sigma_i\,\Sigma_j\,U_{ij}a_i^*a_j^*\mathbf{a}_i\cdot\mathbf{a}_j$.

Final values of the atomic parameters and equivalent isotropic displacement parameters for both compounds appear in Table 2. Final anisotropic displacement parameters and structure amplitudes are given in Tables 3[2] and 4.[2]

X-ray powder diffraction measurements. For phase identification, X-ray powder diffraction patterns of bulk samples were obtained on a Philips powder diffractometer. For unit cell determination, a powder diffraction pattern of a $BaLaCuSe_3$ sample was taken on a Scintag

[1] Indeed, the atomic coordinates for all atoms can be related approximately by such symmetry operations. However, when the structure was refined in space group $Amma$, values of 0.20 for $R_w(F^2)$ (all data) and 0.078 for $R(F)$ ($F_o^2 > 2\sigma(F_o^2)$) and physically unreasonable displacement parameters were obtained. Moreover, of the 664 unique reflections having $k + \ell = 2n + 1$ that would be forbidden in an A-centered lattice, 614 are observed ($F_o^2 > 2\sigma(F_o^2)$). Their average intensity, however, is only one-third of that of those reflections having $k + \ell = 2n$, consistent with the existence of a *pseudo*-A-centered lattice.

[2] See NAPS document No. 05063 for 13 pages of supplementary material. Order from ASIS/NAPS, Microfiche publications, P.O. Box 3513, Grand Central Station, New York, NY 10163. Remit in advance $4.00 for microfiche copy or $7.75 for photocopy. All orders must be prepaid. Institutions and Organizations may order by purchase order. However, there is a billing and handling change for this service of $15. Foreign orders add $4.50 for postage and handling, for the first 20 pages, and $1.00 for additional 10 pages of material, $1.50 for postage of any microfiche orders.

XDS 2000 diffractometer at room temperature. The unit cell dimensions were determined by a least-squares refinement of the *d*-values of 49 uniquely indexed reflections.

UV-visible spectroscopy. Diffuse reflective UV–visible spectra were recorded at room temperature over the wavelength range 190 to 900 nm with a Cary 1E spectrophotometer equipped with a diffuse reflectance accessory. Polytetrafluoroethylene powder (6 mm thick) was used as a reference.

RESULTS AND DISCUSSION

$BaLaCuS_3$ was synthesized both as single crystals and as single-phase polycrystalline samples. It crystallizes in a channel structure type (α). As prepared, $BaLaCuSe_3$ crystallizes in a layered structure (β), but powder diffraction patterns of ground polycrystalline samples revealed the presence of both the α and β phases. The structural features of the α and β phases will be discussed first.

Figures 1 and 2 provide perspective views of these structures. The α structure consists of a three-dimensional framework of LaS_7 monocapped trigonal prisms and CuS_4 tetrahedra. It also exhibits one-dimensional character in the form of channels that extend along the *b* axis. Ba^{2+} ions are accommodated in these channels. In the β structure there are $^2_\infty[LaCuSe_3^{2-}]$ layers separated by Ba^{2+} ions. Figure 3 shows a view of a $^2_\infty[LaCuSe_3^{2-}]$ layer while Fig. 4 shows a polyhedral representation. La atoms are coordinated by six Se atoms at the corners of a distorted octahedron and Cu atoms are coordinated by four Se atoms at the corners of a tetrahedron. The layers are formed by the connection of edge-sharing octahedral chains and corner-sharing tetrahedral chains. β-$BaLaCuSe_3$ is isostructural with Eu_2CuS_3 (i.e., $Eu^{2+}Eu^{3+}Cu^{+}S_3^{2-}$) (20), with La^{3+} ions occupying the same octahedral sites as the Eu^{3+} ions and the Ba^{2+} ions occupying the same seven-coordinate sites as the Eu^{2+} ions.

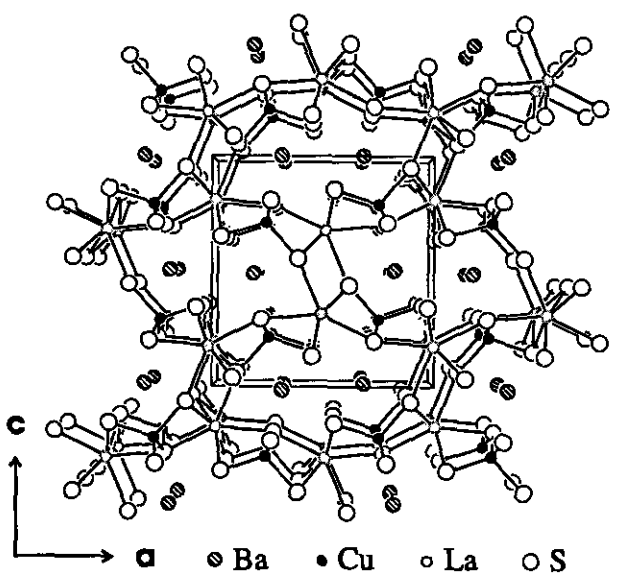

FIG. 1. View along the *b* axis of the $BaLaCuS_3$ or α-$BaLaCuSe_3$ structure.

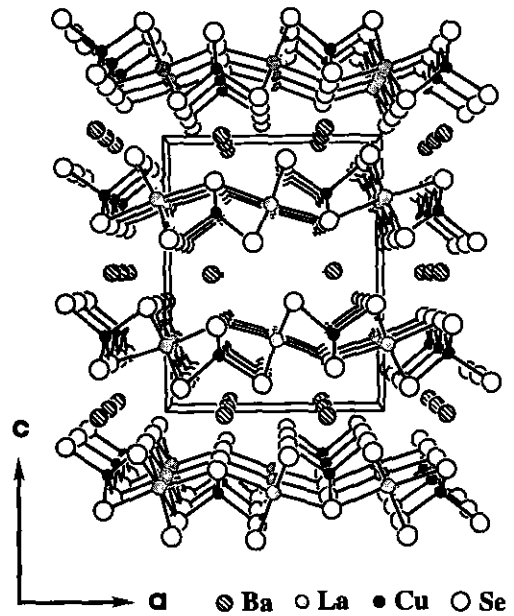

FIG. 2. View along the *b* axis of the β-$BaLaCuSe_3$ structure.

Selected distances and angles for α-$BaLaCuS_3$ and β-$BaLaCuSe_3$ are given in Table 5. In α-$BaLaCuS_3$, the La–S bond lengths range from 2.915(1) to 3.028(1) Å and the Cu–S bond lengths range from 2.338(1) to 2.398(1) Å. In β-$BaLaCuSe_3$, the La–Se bond lengths range from 2.940(2) to 3.019(2) Å and the Cu–Se bond lengths range

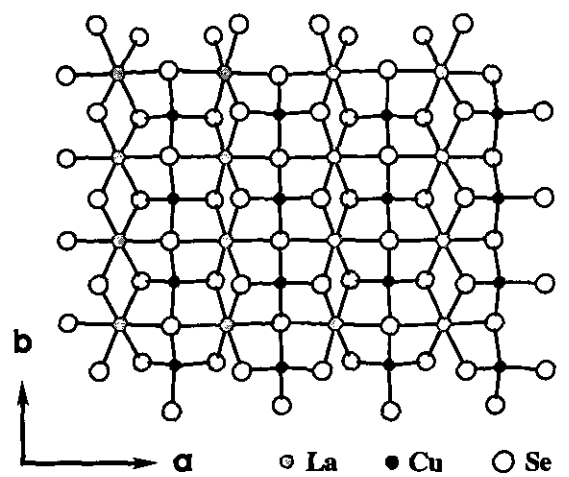

FIG. 3. View along the *c* axis of a $^2_\infty[LaCuSe_3^{2-}]$ layer in β-$BaLaCuSe_3$.

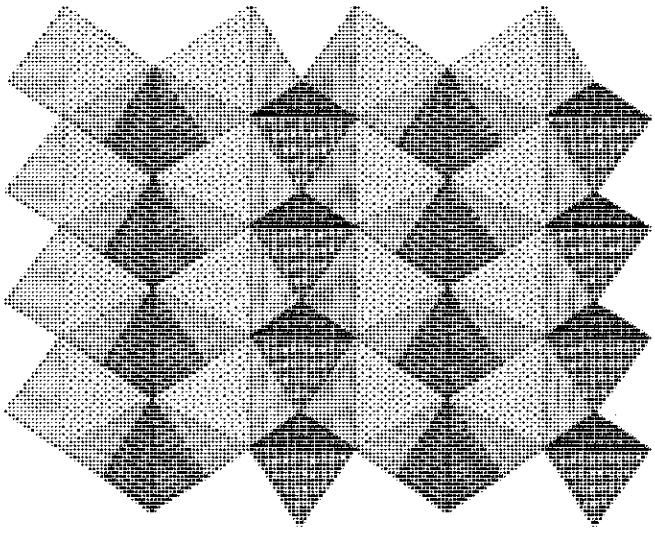

FIG. 4. A polyhedral representation of a $^{2}_{\infty}[LaCuSe_3^{2-}]$ layer in the β-$BaLaCuSe_3$ structure.

from 2.478(2) to 2.577(2) Å. These values compare well with those in the literature. For example, La–S bond lengths vary from 2.898(1) to 3.123(1) Å in $KLaGeS_4$ (8), where La is also seven-coordinated. Octahedrally coordinated La (as in $BaLaCuSe_3$) is uncommon. However, in LaSe, where the La is octahedrally coordinated, the La–Se bond length is 3.024 Å (21) and in La_2SeSiO_4, where the La is eight-coordinate, the La–Se bond lengths range from 3.048(2) to 3.233(2) Å (22). Cu–S bond lengths vary from 2.333(2) to 2.360(2) Å in $K_3Cu_3Nb_2S_8$ (6) and the Cu–Se bond length is 2.456(2) in $K_2CuTaSe_4$ (23). The CuS_4 tetrahedron in the α-$BaLaCuS_3$ structure is close to regular, with S–Cu–S bond angles ranging from 107 to 113°. But in the β-$BaLaCuSe_3$ structure, the $CuSe_4$ tetrahedron is distorted, with Se–Cu–Se angles ranging from 103 to 127°. The $LaSe_6$ octahedron in the β-$BaLaCuSe_3$ structure is slightly distorted with trans-Se–La–Se angles ranging from 174 to 177°. If these polyhedra were regular, the cell would be *A*-centered.

X-ray diffraction patterns were taken from polycrystalline $BaLaCuS_3$ samples. The patterns agree well with that calculated from the crystal structure of α-$BaLaCuS_3$. However, as revealed by powder-diffraction techniques, $BaLaCuSe_3$ undergoes a phase transition that is induced by mechanical grinding. Figure 5 shows a set of X-ray powder diffraction patterns for $BaLaCuSe_3$. Curves (a)

TABLE 5
Selected Bond Lengths (Å) and Bond Angles (deg) in $BaLaCuQ_3$

$BaLaCuS_3$			$BaLaCuSe_3$		
La–S(1)		2.994(2)	La–Se(1)	×2	3.019(2)
La–S(1)		3.000(1)	La–Se(2)		2.940(2)
La–S(2)	×2	2.915(1)	La–Se(2)		2.947(2)
La–S(2)		3.028(1)	La–Se(3)	×2	2.985(2)
La–S(3)	×2	2.942(1)	Ba–Se(1)		3.523(3)
Ba–S(1)	×2	3.167(1)	Ba–Se(1)	×2	3.320(2)
Ba–S(2)	×2	3.230(1)	Ba–Se(2)	×2	3.257(2)
Ba–S(3)		3.118(2)	Ba–Se(3)	×2	3.329(2)
Ba–S(3)	×2	3.178(1)	Cu–Se(1)		2.480(2)
Cu–S(1)	×2	2.372(1)	Cu–Se(2)	×2	2.577(2)
Cu–S(2)		2.398(1)	Cu–Se(3)		2.478(2)
Cu–S(3)		2.338(1)			
S(1)–La–S(1)		148.11(2)	Se(2)–La–Se(2)		174.43(3)
S(1)–La–S(2)		72.83(3)	Se(2)–La–Se(3)	×2	95.48(5)
S(1)–La–S(2)		139.06(3)	Se(2)–La–Se(3)	×2	88.38(5)
S(2)–La–S(1)	×2	78.39(3)	Se(3)–La–Se(3)		91.95(5)
S(2)–La–S(1)	×2	121.20(3)	Se(2)–La–Se(1)	×2	87.29(5)
S(2)–La–S(2)	×2	78.83(3)	Se(2)–La–Se(1)	×2	88.79(5)
S(2)–La–S(2)		93.20(3)	Se(3)–La–Se(1)	×2	177.10(3)
S(2)–La–S(3)	×2	83.28(3)	Se(3)–La–Se(1)	×2	88.64(4)
S(2)–La–S(3)	×2	158.33(3)	Se(1)–La–Se(1)		90.62(5)
S(3)–La–S(1)	×2	78.06(3)	Se(3)–Cu–Se(1)		106.55(7)
S(3)–La–S(1)	×2	79.96(3)	Se(3)–Cu–Se(2)	×2	109.78(6)
S(3)–La–S(2)	×2	124.88(3)	Se(1)–Cu–Se(2)	×2	108.85(6)
S(3)–La–S(3)		92.12(4)	Se(2)–Cu–Se(2)		112.83(7)
S(1)–Cu–S(1)		126.53(5)			
S(1)–Cu–S(2)	×2	103.08(4)			
S(3)–Cu–S(1)	×2	105.19(3)			
S(3)–Cu–S(2)		114.17(4)			

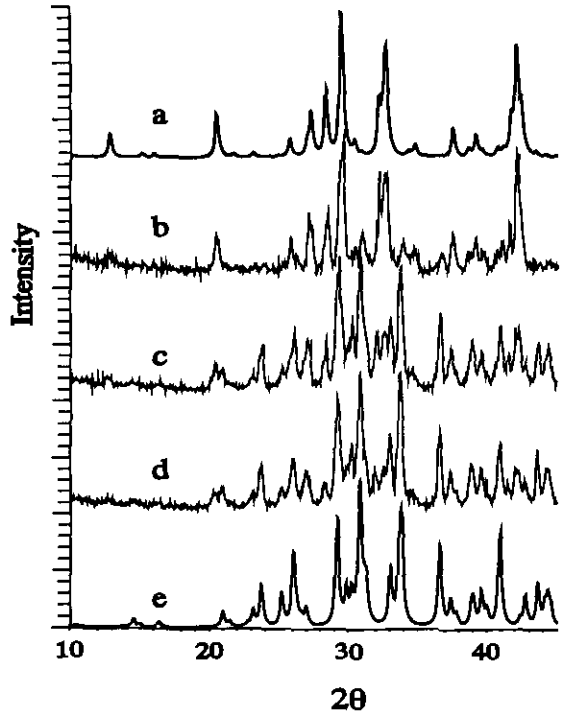

FIG. 5. Calculated and measured X-ray diffraction powder patterns of $BaLaCuSe_3$: (a) calculated for the β phase, (b) measured on an annealed sample, (c) measured on the sample after grinding for 5 min, (d) measured on the sample after grinding for 30 min, and (e) calculated for the α phase.

and (e) are the calculated patterns for the β and α phases, respectively. Curve (b) is from a sample annealed at 600°C for 2 days. This sample was gently crushed, but not ground, before the diffraction pattern was recorded. The β phase predominates. The same sample was then ground manually with an agate mortar and pestle for 5 min. The diffraction pattern (c) now shows the presence of both α and β phases. Grinding of the sample for a total of 30 min increases the proportion of the α phase (curve (d)). Only α-$BaLaCuSe_3$ is observed when the sample is ground for 2 hr with a ball mill (Fritsch Planetary Micromill) with acetone as the mineralizer.[3] The α phase can be transformed to the β phase by annealing at elevated temperatures. While in one experiment annealing an α-sample at 400°C for 12 hr produced a small but noticeable increase in the β phase, annealing at 600°C for 2 days resulted in a complete transition from the α to the β phase. This phenomenon is similar to that reported for $CaCO_3$ (24), in which calcite can be transformed into the metastable high-pressure aragonite phase by grinding. The direction of the phase transition in $BaLaCuSe_3$ is consistent in thermodynamic terms with the calculated density, 6.04 g/cm^3 for α-$BaLaCuSe_3$ compared with 5.81 g/cm^3 for β-$BaLaCuSe_3$. It is likely that α-$BaLaCuSe_3$ is a high-pressure phase that is metastable at ambient pressure, as is aragonite. However, in the absence of thermodynamic data, we cannot exclude the possibility that the high-temperature β phase is metastable at room temperature. Note that the quenched metastable high-temperature phase of ZnS (hexagonal) can be transformed into the more stable cubic phase by grinding at room temperature (25). For both $CaCO_3$ and ZnS, the change in phase becomes noticeable after hours of grinding. For $BaLaCuSe_3$, the phase transition proceeds more rapidly, perhaps because no atom rearrangement is necessary to engender the phase transition. Comparing Figs. 1 and 2, one can see that the channel structure of the α phase can also be viewed as a stack of distorted layers with some La–S bonds across the gaps. Figure 6 shows the local coordination environment of La in α-$BaLaCuS_3$ (b) and β-$BaLaCuSe_3$ (a). The transition from β to corresponds to a distortion of a LaQ_6 octahedron in which the nearly linear diagonal Q–La–Q moiety is bent so as to open up the space necessary for the formation of an additional La–Q bond with a chalcogen atom from an adjacent layer. This results in a monocapped trigonal prismatic geometry about La, as indicated by the thin solid lines. Apparently, the pressure required to effect this transition is provided by the grinding, although grinding may also provide a shear force to assist the kinetic process (26). Efforts to find analogues of $BaLaCuSe_3$ that have the same grinding-induced phase transition were unsuccessful. Among the several other compounds we have synthesized with the β-$BaLaCuSe_3$ structure (27), none exhibits a phase transition after being ground for 15 min. On the other hand, a $BaLaCuS_3$ sample was annealed at 1000°C for 2 days and

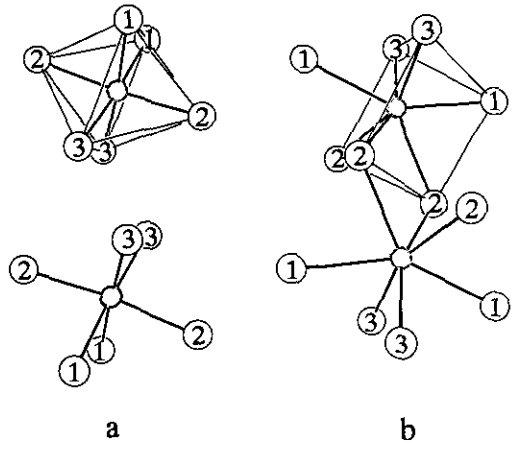

FIG. 6. Coordination geometry around La in (a) β-$BaLaCuSe_3$ and (b) α-$BaLaCuS_3$.

[3] The cell parameters of α-$BaLaCuSe_3$, determined from the X-ray powder pattern at room temperature, are a = 11.800(2), b = 4.408(1), and c = 12.195(2) Å.

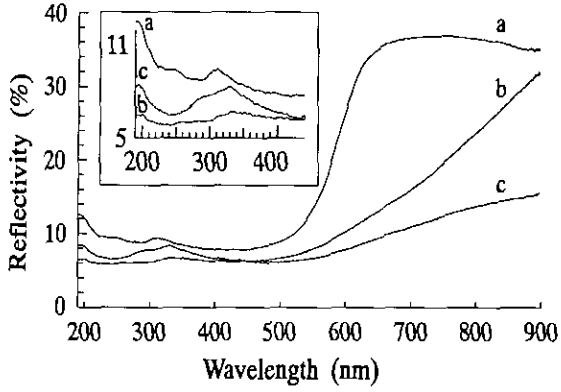

FIG. 7. Diffuse reflective UV–visible spectra of $BaLaCuQ_3$: (a) $BaLaCuS_3$; (b) $BaLaCuSe_3$, primarily the β phase; and (c) α-$BaLaCuSe_3$.

then was quenched in liquid nitrogen. The ensuing powder diffraction pattern showed only the α phase.

Figure 7 shows diffuse reflective UV-visible spectra of $BaLaCuQ_3$. The reflectivity of $BaLaCuS_3$ displays a sharp decrease around 600 nm that corresponds to the absorption edge. The optical band gap, as deduced by a straightforward extrapolation method (28), is 2.00(2) eV. The spectra of the two phases of $BaLaCuSe_3$, however, do not show such sharp transitions. There is structure in the high energy end of all these spectra. Both phases of $BaLaCuSe_3$ have a reflectivity maximum at 330 nm, but there is another maximum at 260 and 300 nm for the β and α phases, respectively. The $BaLaCuS_3$ spectrum has reflectivity maxima at 310 and 250 nm, similar to but blue shifted relative to the spectrum of α-$BaLaCuSe_3$. This shift may be the result of the generally higher bonding energy and ionicity in sulfides compared with selenides. Further understanding of the optical properties of these compounds, however, requires measurements on single crystals and theoretical calculations.

ACKNOWLEDGMENTS

Use was made of the X-ray and scanning electron microscope facilities supported by the National Science Foundation through the Northwestern University Materials Research Center, Grant DMR91-20521. This research was supported by the National Science Foundation through Grant DMR91-14934. We would like to thank Professor Kenneth Poeppelmeier for the use of his ball mill.

REFERENCES

1. Y.-J. Lu and J. A. Ibers, *J. Solid State Chem.* **94,** 381 (1991).
2. P. Wu, Y.-J. Lu, and J. A. Ibers, *J. Solid State Chem.* **97,** 383 (1992).
3. T. D. Brennan and J. A. Ibers, *J. Solid State Chem.* **97,** 377 (1992).
4. P. Wu and J. A. Ibers, *Acta Crystallogr., Sec. C: Cryst. Struct. Commun.* **49,** 126 (1993).
5. Y.-J. Lu and J. A. Ibers, *Inorg. Chem.* **30,** 3317 (1991).
6. Y.-J. Lu and J. A. Ibers, *J. Solid State Chem.* **98,** 312 (1992).
7. M. F. Mansuetto, P. M. Keane, and J. A. Ibers, *J. Solid State Chem.* **101,** 257 (1992).
8. P. Wu and J. A. Ibers, *J. Solid State Chem.* **107,** 347 (1993).
9. S. A. Sunshine, D. A. Keszler, and J. A. Ibers, *Acc. Chem. Res.* **20,** 395 (1987).
10. P. Wu and J. A. Ibers, *Z. Kristallogr.* **208,** 35 (1993).
11. D. Elwell and H. J. Scheel, "Crystal Growth from High-Temperature Solutions." Academic Press, London, 1975.
12. J. D. Carpenter and S.-J. Hwu, *Chem. Mater.* **4,** 1368 (1992).
13. S.-J. Hwu and J. D. Carpenter, *in* Abstracts of Papers—American Chemical Society, 204th National Meeting, Washington, DC, INOR 393, ACS, Washington, DC, 1992.
14. A. W. Sleight, *Inorg. Synth.* **14,** 155 (1974).
15. R. Riccardi, C. Sinistri, G. V. Campari, and A. Magistris, *Z. Naturforsch., A: Astrophys. Phys. Phys. Chem.* **25,** 781 (1970).
16. J. C. Huffman, unpublished work.
17. G. M. Sheldrick, SHELXTL PC Version 4.1, An Integrated System for Solving, Refining, and Displaying Crystal Structures from Diffraction Data. Siemens Analytical X-Ray Instruments, Inc., Madison, WI.
18. G. M. Sheldrick, SHELXL-92 Unix Beta-test version.
19. Y. Le Page, *J. Appl. Crystallogr.* **20,** 264 (1987).
20. P. Lemoine, D. Carré, and M. Guittard, *Acta Crystallogr., Sect. C: Cryst. Struct. Commun.* **42,** 390 (1986).
21. M. Guittard and A. Benacerraf, *C. R. Hebd. Séances Acad. Sci* **248,** 2589 (1959).
22. T. D. Brennan and J. A. Ibers, *Acta Crystallogr., Sect. C: Cryst. Struct. Commun.* **47,** 1062 (1991).
23. Y.-J. Lu, P. Wu, and J. A. Ibers, *Eur. J. Solid State Inorg. Chem.* **30,** 101 (1993).
24. J. H. Burns and M. A. Bredig, *J. Chem. Phys.* **25,** 1281 (1956).
25. T. Sekine and Y. Kotera, *J. Lumin.* **12/13,** 929 (1976).
26. V. V. Boldyrev, *J. Chim. Phys. Phys.-Chim. Biol.* **83,** 821 (1986).
27. P. Wu, A. E. Christuk, and J. A. Ibers, *J. Solid State Chem.* **110,** 337 (1994).
28. O. Schevciw and W. B. White, *Mater. Res. Bull.* **18,** 1059 (1983).
29. J. C. Huffman, Ph.D. thesis, Indiana University, 1974.
30. J. de Meulenaer and H. Tompa, *Acta Crystallogr.* **19,** 1014 (1965).